ISSN 1009 – 3095 *Journal of Zhejiang University SCIENCE* V.4, No.1, P.21 – 27, Jan. – Feb., 2003
http://www.periodicals.com.cn; http://www.zju.edu.cn/English
http://www.zjupress.com; http://lib.zju.edu.cn/eindex.htm; jzu_s@mail.hz.zj.cn

Three-dimensional nonlinear flutter analysis of long-span suspension bridges during erection*

ZHANG Xin-jun(张新军)[1†], SUN Bing-nan(孙炳楠)[1], XIANG Hai-fan(项海帆)[2]

([1] *Department of Civil Engineering, Zhejiang University, Hangzhou 310027, China*)
([2] *Department of Bridge Engineering, Tongji University, Shanghai 200092, China*)

[†]E-mail: xinjunzh@163.com
Received Dec.5, 2001; revision aeceptel June 8, 2002

Abstract: In this work, the aerodynamic stability of the Yichang Suspension Bridge over Yangtze River during erection was determined by three-dimensional nonlinear flutter analysis, in which the nonlinearities of structural dynamic characteristics and aeroelastic forces caused by large deformation are fully considered. An interesting result obtained was that the bridge was more stable when the stiffening girders were erected in a non-symmetrical manner as opposed to the traditional symmetrical erection schedule. It was also found that the severe decrease in the aerodynamic stability was due to the nonlinear effects. Therefore, the nonlinear factors should be considered accurately in aerodynamic stability analysis of long-span suspension bridges during erection.

Key words: Long-span suspension bridges, Nonlinear flutter analysis, Erection stage
Document code: A **CLC number:** U448.25

INTRODUCTION

It has been recognized that long-span bridges, cable-supported bridges in particular, are subject to the dynamic wind action. The aerodynamic stability (flutter) of suspension bridges during erection is a subject of major concern for researchers and engineers. Although the period of construction is usually not too long and the design wind speed can hence be reduced to a lower value than that in the final state, the stiffening girder of suspension bridges during erection lacks torsional continuity, which contributes to the reduction of the ratio between the dominant torsional and vertical frequencies, and weaken the aerodynamic stability during erection. Thus, it is now common knowledge that, regarding aerodynamic stability, construction condition is often less favorable than that in the final state.

During the last 30 years, many researchers (Brancaleoni, 1992; Larsen, 1995; Tanaka et al., 1996, 1998, 1999; Diego Cobo del Arco, 1999a, 1999b, 2001) studied the aerodynamic stability of suspension bridges in erection. Some methods for improving the aerodynamic stability of suspension bridges during erection were also discussed. But their researches were mainly based on linear theory, that is to say, the analyses were based on the undeformed structures. For long-span suspension bridges in erection, total structural stiffness is much lower and large deformation occurs due to the dynamic wind action. The large deformation, on the one hand, will affect structural stiffness and the dynamic characteristics. On the other hand, the aerodynamic shapes will be changed remarkably, which lead to significant variation of the wind forces acting on the bridges. Therefore, it is essential to established nonlinear analytical approach to investigate the actual aerodynamic behaviors of long-span suspension bridges in erection.

NONLINEAR FLUTTER THEORY AND COMPUTING PROCEDURE

1. Nonlinear aerostatic and aerodynamic force models

Generally, wind-structure interaction is treated as the action of aerostatic and aerodynamic effects. The wind action changes significantly the bridge configuration, and the resulting deformation will inversely change the aerostatic and aerodynamic forces acting on the bridges. So

* Project supported by National Natural Science Foundation of China (No.598954410), and China Postdoctoral Science Foundation (No.2002031245)

the wind-structure interaction is a nonlinear function of structural deformation.

The aerostatic effect is usually treated as the resultant of 3 aerostatic components of wind force acting on the bridge: the drag force, lift force and pitch moment as shown in Fig.1. The aerostatic force acting on per unit length of the bridge deck can be expressed as follows:

$$\begin{aligned} F_z &= \frac{1}{2} \cdot \rho U^2 \cdot D \cdot C_z(\alpha) \\ F_y &= \frac{1}{2} \cdot \rho U^2 \cdot B \cdot C_y(\alpha) \\ M_x &= \frac{1}{2} \cdot \rho U^2 \cdot B^2 \cdot C_M(\alpha) \end{aligned} \tag{1}$$

where ρ is the air density; U is the mean velocity at the bridge deck level; D is the bridge deck height; B is the bridge deck width; $C_z(\alpha)$, $C_y(\alpha)$, and $C_M(\alpha)$ are the aerostatic coefficients obtained from the section model tests; α is the effective angle of attack including the initial attack angle θ_0 and the additional attack angle θ caused by the torsional deformation.

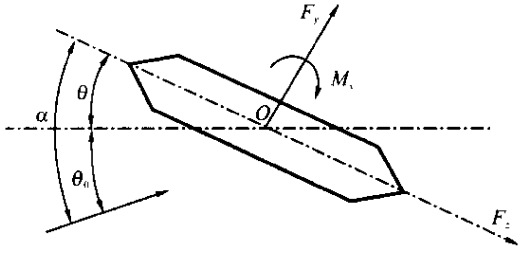

Fig.1 Aerostatic force acting on the deck

The aerodynamic force is generally assumed to be composed of: (1) the self-excited force due to the dynamic wind-structure interaction in the smooth oncoming wind flow; (2) the buffeting force due to turbulence in the oncoming wind flow. The buffeting force does not make the system aerodynamically unstable, so it is usually neglected in flutter analysis. The self-excited aerodynamic force includes self-excited lift, L_h, and drag, D_p, forces as well as the aerodynamic moment, M_α represented by the 18 flutter derivatives as (Jain, 1996):

$$\begin{aligned} L_h = \frac{1}{2}\rho U^2(2B)\Big[& KH_1^* \frac{\dot{h}}{U} + KH_2^* \frac{B\dot{\alpha}}{U} + \\ & K^2 H_3^* \alpha + K^2 H_4^* \frac{h}{B} + KH_5^* \frac{\dot{p}}{U} + K^2 H_6^* \frac{p}{B}\Big] \\ D_p = \frac{1}{2}\rho U^2(2B)\Big[& KP_1^* \frac{\dot{p}}{U} + KP_2^* \frac{B\dot{\alpha}}{U} + \\ & K^2 P_3^* \alpha + K^2 P_4^* \frac{p}{B} + KP_5^* \frac{\dot{h}}{U} + K^2 P_6^* \frac{h}{B}\Big] \\ M_\alpha = \frac{1}{2}\rho U^2(2B^2)\Big[& KA_1^* \frac{\dot{h}}{U} + KA_2^* \frac{B\dot{\alpha}}{U} + \\ & K^2 A_3^* \alpha + K^2 A_4^* \frac{h}{B} + KA_5^* \frac{\dot{p}}{U} + K^2 A_6^* \frac{p}{B}\Big] \end{aligned} \tag{2}$$

where H_i^*, A_i^*, P_i^* $(i = 1-6)$ are the experimentally determined flutter derivatives which are dependent on the reduced frequency $K(=B\omega/U)$ and the effective attack angle α, ω is the response angular frequency.

Eq.(2) represents the aerodynamic force acting on per unit length of the bridge deck. To convert these uniformly distributed force into member end effects, a simple lumping procedure is adopted whereby one-half of the force is assumed to act at each member end. Using a space frame element idealization of the overall bridge, the equivaleut aerodynamic joint load, $\{F\}$, is subdivided into stiffness component $[A_s]$ and damping component $[A_d]$ as

$$\{F\} = \frac{1}{2}\rho U^2\Big[[A_s]\{q\} + \frac{1}{U}[A_d]\{\dot{q}\}\Big] \tag{3}$$

where $\{q\}$, $\{\dot{q}\}$ are displacement and velocity vectors; $[A_s]$, $[A_d]$ are the aerodynamic stiffness and damping matrices.

2. Nonlinear flutter analysis

The nonlinear flutter analysis in this paper includes two steps: (1) aerostatic analysis to predicate the equilibrium state, which is the initial state of oscillation; (2) aerodynamic response analysis of the deformed bridge structures.

The static equilibrium state of a bridge structure under a certain wind speed must be solved by the iteration approach due to its double nonlinearity of structural and aerostatic force. The iteration equation can be expressed as (Boonyapinyo, 1994):

$$\begin{aligned} &([K_E]_{j-1} + [K_\sigma]_{j-1})\{\Delta\delta_j\} = \\ &\{F_j(\alpha_j)\} - \{F_{j-1}(\alpha_{j-1})\} \end{aligned} \tag{4}$$

where $[K_E]_{j-1}$ and $[K_\sigma]_{j-1}$ are the linear-elastic stiffness matrix and geometrical matrix respectively; $\{F_{j-1}(\alpha_{j-1})\}$ and $\{F_j(\alpha_j)\}$ are the wind load vectors corresponding to the effective

attack angle α_{j-1} in step $j-1$ and α_j in step j under the wind speed of U.

The Euclidean Norm of the aerodynamic static coefficients of lift, drag and pitch moment is taken as convergence criterion, which can be expressed as:

$$\left\{\frac{\sum_{l}^{N_a}[C_K(\alpha_j)-C_k(\alpha_{j-1})]^2}{\sum_{l}^{N_a}[C_K(\alpha_{j-1})]^2}\right\}^{\frac{1}{2}} \leqslant \varepsilon_k \quad (K \text{ represents } L,\ D,\ M) \tag{5}$$

where ε_K is the prescribed convergence accuracy; N_a is the total number of the nodes subjected to the wind force.

When the aerostatic equilibrium state is found, aerodynamic response analysis can then be performed on the deformed bridge configuration. For a structural system with n discreet degrees of freedom, the equation of motion due to the self-excited aerodynamic force can be expressed as

$$[M]\{\ddot{q}(x,t)\}+[D]\{\dot{q}(x,t)\}+[K]\{q(x,t)\}=\frac{1}{2}\rho U^2\left([A_s]\{q(x,t)\}+\frac{1}{U}[A_d]\{\dot{q}(x,t)\}\right) \tag{6}$$

where $[M]$, $[D]$ and $[K]$ are the global structural mass, damping and tangent stiffness matrices; $[A_s]$, $[A_d]$ are the global structural aerodynamic stiffness and damping matrices.

Modal analysis is used here to solve the Eq.(6). For dynamic motion, the response at all degree is separated into spatial (natural modes) and time-dependent (generalized coordinates) components as

$$\{q(x,t)\}=[\phi]\{\xi(t)\} \tag{7}$$

where $[\phi]$ is an n-row by m-column matrix of natural mode shapes (the ith column corresponding to the ith natural mode); $\{\xi(t)\}$ is an m-row generalized coordinates vector; n is the total degrees of freedom, m is the number of modes in the response.

Since flutter response is typically harmonic, the generalized coordinate can be assumed to be a damped, harmonic form and represented along the complex plane as

$$\{\xi(\boldsymbol{t})\} = \{\boldsymbol{R}\}\exp(\lambda \boldsymbol{t}) \tag{8}$$

where $\{R\}$ is the response amplitude; $\lambda=(\delta+\mathrm{i})\omega$; δ is the response logarithmic decrement; ω is the angular frequency of response; $\mathrm{i}=\sqrt{-1}$.

Substituting Eq.(7) and Eq.(8) into Eq.(6), then pre-multiplying the transpose of the natural mode matrix $[\phi]$, considering the orthoganality between modes and existence of a nontrivial solution, yields a determinant as follows:

$$\left|[M^g]\left(\frac{U}{B}\right)^2 p^2+[D^g]\left(\frac{U}{B}\right)p+[K^g]-\frac{1}{2}\rho U^2\left[[A_s^g]+\frac{1}{B}[A_d^g]iK\right]\right|=0 \tag{9}$$

where $[M^g]=[\phi]^{\mathrm{T}}[M][\phi]$, $[D^g]=[\phi]^{\mathrm{T}}[D][\phi]$, $[K^g]=[\phi]^{\mathrm{T}}[K][\phi]$ are the generalized mass, damping and stiffness matrices; $[A_s^g]=[\phi]^{\mathrm{T}}[A_s][\phi]$, $[A_d^g]=[\phi]^{\mathrm{T}}[A_d][\phi]$ are the generalized aerodynamic stiffness and damping matrices; $\boldsymbol{P}=\boldsymbol{K}(\delta+\mathbf{i})$, $\boldsymbol{K}=\boldsymbol{B}\omega/\boldsymbol{U}$.

For a given wind speed $\boldsymbol{U}$, the Eq.(9) can be solved by the PK-F method (Namini, 1992), the value p that makes the determinant equal to zero gives the actual oscillation response. The logarithmic decrement and angular frequency of response can be computed as

$$\delta=\frac{Re(p)}{Im(p)},\quad \omega=\frac{\boldsymbol{U}}{\boldsymbol{B}}Im(p) \tag{10}$$

where Re and Im are the real and imaginary parts of a complex variable respectively.

According to the logarithmic decrement, the response can be defined to be: $\delta<0$, stable; $\delta=0$, flutter critical condition; $\delta>0$, unstable.

3. Computational procedure

Based on the above method a computer program BSNFA (developed by Zhang, 2000) was developed for aerodynamic stability analysis of suspension bridges during erection. The computation of the flow is described as follows:

(1) Input bridge finite element model, flutter derivatives and aerostatic coefficients etc.

(2) For each erection stage, determine the equilibrium state under the corresponding dead loads by removing the units that have not been hoisted into position and also removing the percentage of dead load that is placed after the closing of the deck.

(3) Calculate the current wind speed: $U=$

$U_{low} + U_{inc}$, where U_{low} is the lowest computed wind speed and U_{inc} is the increment of wind speed.

(4) Perform structural nonlinear aerostatic analysis under the current wind speed U to obtain the aerostatic equilibrium state.

(5) On the post-deformed aerostatic equilibrium state, perform the dynamic characteristic analysis, select the modes that participate in flutter analysis and establish the matrix of modes $[\phi]$.

(6) Taking into consideration the deformation obtained in step 4, calculate the self-excited aerodynamic force acting on the bridges. A solution predicting the status of response can be obtained by using the PK-F method.

(7) Determine the dynamic response according to the logarithmic decrement δ. If $\delta < 0$, flutter critical condition is not reached, then return to step 3, repeat step 4 – 6 and perform the above analysis under the increased wind speed. The analytical procedure is continued until the flutter critical condition is reached.

Step 4 describes the flow of structural nonlinear aerostatic analysis as follows:

1) Calculate the aerostatic load $\{F_0\}$ under the initial attack angles of the previous aerostatic equilibrium state, fixing: $\{F_2\} = \{F_0\}$, $\{F_1\} = \{0\}$;

2) Calculate the aerostatic load increment $\{\Delta F\} = \{F_2\} - \{F_1\}$, let $\{F_1\} <= \{F_2\}$;

3) Perform structural geometric nonlinear analysis under the incremental aerostatic load, the changed equilibrium position is then obtained;

4) Determine the effective wind attack angles of the deck, then calculate the changed aerostatic load $\{F_2\}$;

5) Determine the convergence criterion as described in Eq.(5). If the solution is not convergent, then return to step 2, repeat step 2 – 4 until convergence is reached.

AERODYNAMIC STABILITY ANALYSIS DURING ERECTION

1. Description of the Yichang Suspension Bridge

The Yichang Bridge over the Yangtze River is a suspension bridge with main span of 960 m. The bridge deck is a streamlined deck girder with width of 30 m and height of 3 m. The proposed erection sequence for the center span is to start from the midspan and extend alternatively towards both pylons. Initially, the box segments are connected with temporary hinges which allow the full transfer of torsional and lateral stiffness while the vertical bending is left free. They are not welded together until all the segments are in position.

The full-model wind tunnel tests of the Yichang Bridge during erection was done at the State Key Laboratory of Disaster Reduction in Civil Engineering at Tongji University (1999). In order to compare the analytical results with the tests, seven erection stages which is very close to the test cases are selected for the aerodynamic stability analysis in this paper. The erection ratios and length of bridge deck erected at each erection construction stage are presented in Table 1.

Table 1 Erection ratio and length of bridge deck erected

Erection stage	1	2	3	4	5	6	7
Erection length(m)	84.4	180.9	277.4	466.2	566.8	759.8	960.0
Erection ratio(%)	8.8	18.8	28.9	46.5	59.0	79.0	100

The finite element model of the Yichang Suspension Bridge was formed with spatial geometrically nonlinear beam and bar elements. The stiffening girder, towers and rigid beam linking the stiffening girder and hangers were idealized to spatial beam elements, the hangers and main cables were idealized to spatial bar elements. The finite element idealized model in the final state was shown in Fig.2. The aerostatic coeffi-

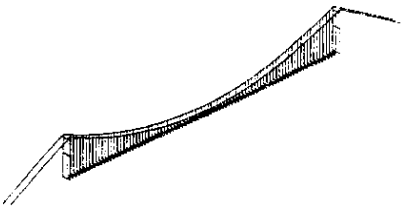

Fig.2 The finite element model of Yichang Suspension Bridge in the final state

cients and flutter derivatives A_i^*, $H_i^T(i=1,4)$ in erection and final state were obtained from wind tunnel section-model tests. Structural damping was taken as $\xi_h = \xi_\alpha = 0.5\%$.

2. Bridge deck erected symmetrically

In the case of bridge deck erected symmetrically, the segments are erected in two directions simultaneously from midspan to the pylons as shown in Fig.3. The first symmetric vertical bending frequency (f_h) and torsional frequency (f_α) at different erection stages are plotted in Fig.4, where they were compared to the results obtained from tests. Generally, good agreement was achieved between the two cases. The ratio f_α/f_h varying with the erection process is plotted in Fig.5, which is also very close to the test results.

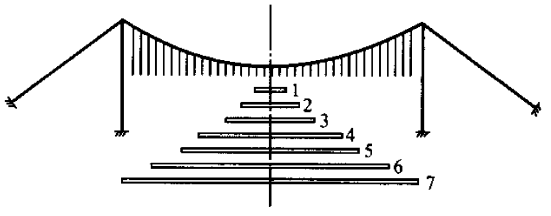

Fig.3 Bridge deck erected symmetrically

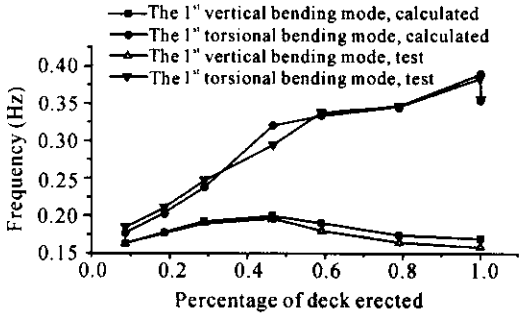

Fig.4 Evolution of the first vertical and torsional frequencies

The vertical bending frequency changes little during erection. For long-span suspension bridges, the vertical bending stiffness is provided mostly by the main cables. Particularly during the deck erection with the initial joining of the girder segments by temporary hinges, the hoisted deck segments add weight but hardly influence the vertical bending stiffness. On the contrary, the torsional frequency increases remarkably as

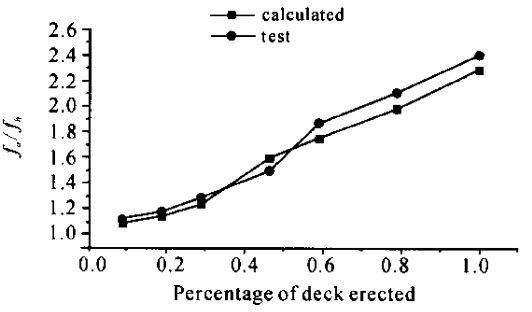

Fig.5 Evolution of the ratio f_α/f_h

the erection proceeds. In torsional oscillation, two main cables oscillate adversely in the cable plane, the restraint against mutual twisting of cables is given mainly by the cables themselves. The stiffness of cables increases as the erection proceeds, the restraint against torsional oscillation is added consequently. As a result, the ratio f_α/f_h increases gradually as the erection proceeds due to the increase of the torsional frequency.

Fig.6 presents the evolution of flutter speed obtained analytically and the aeroelastic full model test at 0° wind angle of incidence.

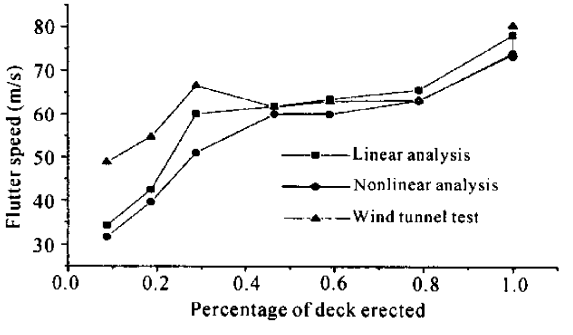

Fig.6 Evolution of flutter speed

In the early stages, there were some differences between the two cases. but the analytical results were very similar to the experimental results after about 40% of the bridge deck had been erected. The difference between the analytical and experimental results is mainly caused by the fact that the calculated dynamic characteristics differ somewhat from the experimental ones. In additional, structural damping of the model is really different from the values simply assumed in the numerical calculation. Before 30% of the deck was erected, aerodynamic instability was

encountered because of the low flutter speeds. But after that, the flutter speed increased rapidly and exceeded 50 m/s, no aerodynamic stability problems existed. The flutter speed increased rapidly at the early stages, but slowly at the later stages. The increase of flutter speed could be mainly contributed was due to the increase of the torsional frequency and also the modal coupling as seen in Table 2. In the early three stages, the flutter mode was composed of the first vertical and torsional modes. But at the later stages, the second symmetric mode participated in the flutter.

Table 2 Main modes participating in the flutter

Erection stage	1	2	3	4	5	6	7
Modes	1-S-V	1-S-T	1-S-V	1-S-V	1-S-V	1-S-V	1-S-V
	1-S-T	1-S-T	1-S-T	1-S-T	1-S-T	1-S-T	1-S-T
				2-S-V	2-S-V	2-S-V	2-S-V

Note: S-symmetric; V-vertical; T-torsional

Comparison of the results obtained from linear flutter analysis and nonlinear analysis showed that the nonlinear factors decreased the flutter speed by 1 m/s to 9 m/s. The decreased flutter speed was mainly caused by the increased wind attack angle due to the large torsional deformation. The increased wind attack angle increased the effective angle between the deck and oncoming flow, and blunted the streamlined shape, and consequently decreased the aerodynamic stability of the bridge.

3. Bridge deck erected non-symmetrically

In order to investigate the effect of the erection sequence on the aerodynamic stability of long-span suspension bridges, the case of bridge deck erected non-symmetrically was studied. Fig. 7 shows the configuration of bridge deck-erected non-symmetrically. The ratio of eccentricity is defined by Δ/L_e, where Δ is the distance between the center of the erected deck and the midspan, which shows the degree of eccentricity in deck distribution; L_e is the length of the erected deck.

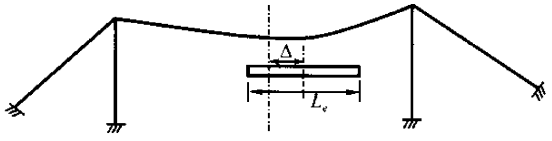

Fig.7 Bridge deck erected non-symmetrically

Linear and nonlinear flutter analysis were performed from stage 1 to stage 5 with different ratio of eccentricity. Fig. 8 shows the flutter speed for different ratio of eccentricity.

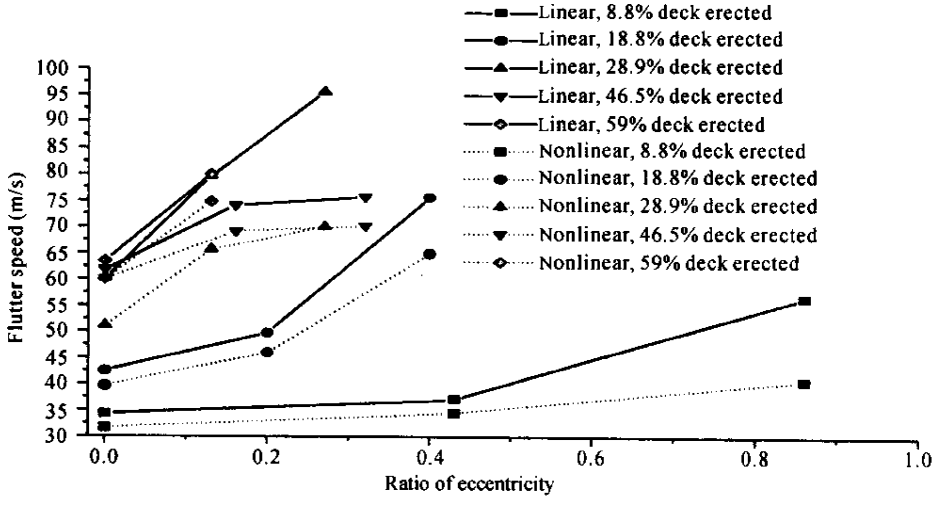

Fig.8 Flutter speed changing with the ratio of eccentricity

An important increase in the flutter speed can be achieved using non-symmetric erection sequence as compared to the traditional symmetric erection sequence. The increase of flutter speed can be attributed, on the one hand, to the higher torsional frequencies compared to those in the case of bridge deck erected symmetrically. On the other hand, the coupling between the torsional and vertical modes being slightly weaker compared to the case of bridge deck erected symmetrically allows more modes to participate in the flutter.

Comparison of linear analysis and nonlinear analysis, results showed that the effect of nonlinear factors on flutter speed was more significant than in the symmetric case. With increasing the eccentricity of deck erection, the flutter speed decreased significantly. From the linear results the amplitude ranged from 3 m/s to 16 m/s at all the cases. Furthermore, in erection stage 2 (when the ratio of eccentricity reached 0.4) and erection stage 3 (when the eccentricity ratio reached 0.27), flutter instability was not observed, but aerostatic divergence occurred. Like-wise, the decreasing flutter speed could be also attributed to the larger effective wind attack angle due to the torsional deformation, which made the streamline aerodynamic shape of the deck more bluff, the aerodynamic stability and further decrease. Therefore, the nonlinear factors should be considered in this case.

CONCLUSIONS

3D nonlinear flutter analytical method was used to the aerodynamic stability analyses for the erection process of the Yichang Suspension Bridge over Yangtze River. The cases of bridge deck erected symmetrically and non-symmetrically were studied. The aerodynamic stability was bad at the early erection stages, but improved rapidly at the later stage of the erection process. An interesting result obtained was that the bridge was more stable when the deck was erected in a non-symmetrical sequence as opposed to the traditional symmetrical erection sequence. So the non-symmetrical erection sequence is an effective means to improve the aerodynamic stability of long-span suspension bridges during erection, particularly at the early erection stages. The effect of nonlinear factors on the aerodynamic stability of long-span suspension bridges in erection is important. It leads to the great decrease of flutter speed. Therefore, the nonlinear factors should be considered in the aerodynamic stability analysis of long-span suspension bridges during erection.

References

Boonyapinyo, V., Yamada, H. and Miyata, T., 1994. Wind-induced nonlinear lateral-torsional buckling of cable-stayed bridges. *J. Struct. Engrg., ASCE*, **120**(2): 486 – 506.

Brancaleoni, F., 1992. The construction phase and its aerodynamic issues. *In*: Aerodynamics of Large Bridges, A. Larsenced., Balkema, Rotterdam, the Netherlands. p.147 – 158.

Cobo del Arco, D., 1999a. Improving the wind stability of box-girder suspension bridges in erection. *In*: Wind Engineering into 21st Century, Balkema, Rotterdam, the Netherlands, p.857 – 862.

Cobo del Arco, D., 1999b. Improving suspension bridge wind stability with aerodynamic appendages. *J. Struct. Engrg., ASCE*, **125**(12): 1367 – 1375.

Cobo del Arco, D., 2001. Improving the wind stability of suspension bridges during construction. *J. Struct. Engrg., ASCE*, **127**(8): 869 – 875.

Jain, A., Jones, N.P. and Scanlan, R.H., 1996. Coupled flutter and buffeting analysis of long span bridge. *J. Struct. Engrg. ASCE* **122**(7): 716 – 725.

Larsen, A., 1995. Prediction of aeroelastic stability of suspension bridges during erection. Proceeding of 9th International Conference on Wind Engineering New Delhi, p.917 – 927.

Namini, A.H. 1992. Finite element-based flutter analysis of cable-suspended bridge. *J. Struct. Engrg., ASCE*, **118**(6): 1509 – 1526.

Tanaka, H. Damsgaard, A. and Reino, p., 1996. Aerodynamic stability of a suspension bridge with a partially constructed bridge deck. 15th IABSE Congress Report, Lisbon, Portugal, p.113 – 118.

Tanaka, H., 1998. Aerodynamics of long-span bridges during erection. *In*: Bridge Aerodymics, A. Larsen & S. Esdah(eds), A.A. Balkema, Rotterdam, the Netherlands, p.119 – 127.

Tanaka, H. and Gimsing, N.J., 1999. Aerodynamic stability of non-symmetrically erected suspension bridge girders. *J. Wind Engrg. Indust. Aerodyn.*, **80**: 85 – 104.

Xiang, H. F., 1999. Wind-resistant research Report of Yichang Bridge Yangtze River During Erection. Res. Rep. of Tongji University, Shanghai (in Chinese).

Zhang, X. J., 2000. Three-dimensional nonlinear flutter analysis of long-span bridges. Ph. D. Dissertation. Tongji University, Shanghai, China (in Chinese).